Mon. Not. R. Astron. Soc. **365,** 1300–1308 (2006) doi:10.1111/j.1365-2966.2005.09812.x

Minimal models of cooling neutron stars with accreted envelopes

A. D. Kaminker,[1⋆] M. E. Gusakov,[1⋆] D. G. Yakovlev[1⋆] and O. Y. Gnedin[2⋆]
[1]*Ioffe Physical Technical Institute, Politekhnicheskaya 26, 194021 Saint-Petersburg, Russia*
[2]*Ohio State University, Department of Astronomy, 140W 18th Avenue, Columbus, OH 43210, USA*

Accepted 2005 November 1. Received 2005 September 23; in original form 2005 March 28

ABSTRACT

We study the 'minimal' cooling scenario of superfluid neutron stars with nucleon cores, where the direct Urca process is forbidden and enhanced cooling is produced by neutrino emission due to the Cooper pairing of neutrons. Extending our recent previous work, we include the effects of surface accreted envelopes of light elements. We employ the phenomenological density-dependent critical temperatures $T_{\rm cp}(\rho)$ and $T_{\rm cnt}(\rho)$ of singlet-state proton and triplet-state neutron pairing in a stellar core, as well as the critical temperature $T_{\rm cns}(\rho)$ of singlet-state neutron pairing in a stellar crust. We show that the presence of accreted envelopes simplifies the interpretation of observations of thermal radiation from isolated neutron stars in the scenario of our recent previous work and widens the class of models for nucleon superfluidity in neutron star interiors consistent with the observations.

Key words: stars: evolution – stars: neutron.

1 INTRODUCTION

New observations of thermal radiation from isolated middle-aged neutron stars (e.g. Pavlov, Zavlin & Sanwal 2002; Pavlov & Zavlin 2003) have initiated further development of the cooling theory of these objects. Its main aim is to interpret the data and constrain the still poorly known properties of dense matter in neutron star cores, such as composition, the equation of state and nucleon superfluidity (e.g. Yakovlev & Pethick 2004; Page et al. 2004, and references therein).

It is well known (e.g. Yakovlev & Pethick 2004) that theoretical models of non-superfluid neutron stars, which possess nucleon cores and cool via the modified Urca process of neutrino emission, cannot explain the observations. Some neutron stars (e.g. RX J0822−4300 and PSR B1055−52) are much warmer than predicted by these theories, while others (e.g. the Vela pulsar or the compact source in CTA 1) are much colder. The warmest objects can be treated as relatively low-mass neutron stars with strong proton (e.g. Kaminker, Haensel & Yakovlev 2001) or neutron (e.g. Gusakov et al. 2004b) pairing in their cores. Strong pairing suppresses the modified Urca process and makes the stars warmer. The coldest stars should have higher neutrino emission than the emission provided by the modified Urca process. They are usually treated as massive neutron stars, which cool either via the powerful direct Urca process in nucleon (or nucleon/hyperon) matter or via similar processes in kaon-condensed, pion-condensed, or quark matter in their inner cores.

Recently Page et al. (2004) and Gusakov et al. (2004a) proposed new scenarios of neutron star cooling which involve only standard physics of neutron star interiors. The neutron star cores are assumed to contain nucleons (no exotic forms of matter) with the forbidden direct Urca process. Some enhancement of the cooling can be provided by neutrino emission due to Cooper pairing of nucleons. Page et al. (2004) called their cooling scenario the 'minimal cooling model' (for its simplicity). We will also use this very properly chosen name for the scenario of Gusakov et al. (2004a) that is based on the same assumptions (but differs in their realization; see below).

According to our previous paper (Gusakov et al. 2004a), enhanced cooling is produced by neutrino emission due to Cooper pairing of neutrons in the cores of massive neutron stars, while the warmest objects are thought to be low-mass stars with strong proton pairing in their cores. We assumed a phenomenological model of strong density-dependent singlet-state proton pairing with the critical temperature $T_{\rm cp}(\rho)$, which has maximum value $T_{\rm cp}^{\rm max} \gtrsim 5.0 \times 10^9$ K. We also assumed a phenomenological model of moderate triplet-state neutron pairing $T_{\rm cnt}(\rho)$ with maximum critical temperature $T_{\rm cnt}^{\rm max} \sim 6.0 \times 10^8$ K shifted to higher ρ, where proton pairing dies out. We were able to interpret all the data but under stringent constraints on the density dependence of $T_{\rm cnt}(\rho)$.

The present paper extends our previous analysis. We use the same equation of state of matter in neutron star interiors (Douchin & Haensel 2001) and the same model of triplet-state neutron pairing. However, in addition, we take into account the effects of surface layers of light (accreted) elements (H and/or He), as well as singlet-state neutron pairing $T_{\rm cns}(\rho)$ in the stellar crust. The effects of accreted envelopes allow us to lower the proton pairing ($T_{\rm cp}^{\rm max} \gtrsim 10^9$ K) required to explain the data. This weaker proton pairing is consistent with recent microscopic calculations of proton critical temperatures by Zuo et al. (2004) and Takatsuka & Tamagaki (2004) [although some other calculations predict much stronger proton pairing – e.g. Lombardo & Schulze (2001), and see also references in Yakovlev,

⋆E-mail: kam@astro.ioffe.ru (ADK); gusakov@astro.ioffe.ru (MEG); yak@astro.ioffe.ru (DGY); ognedin@astronomy.ohio-state.edu (OYG)

Levenfish & Shibanov (1999) and the recent paper by Tanigawa, Matsuzaki & Chiba (2004)].

Let us emphasize the difference between the cooling scenarios of Page et al. (2004) and Gusakov et al. (2004a). In particular, Page et al. (2004) used several selected models of triplet-state neutron pairing provided by microscopic theories. The corresponding cooling curves do not depend sensitively on neutron star mass and do not allow the authors to explain all the data in the frame of one physical model of neutron star interiors. In contrast, Gusakov et al. (2004a) used phenomenological models of triplet-state pairing and succeeded in explaining all the data (although under stringent constraints on these models; see their paper for details). Note that Page et al. (2004) analysed the effect of accreted envelopes on their minimal cooling models, but our models are different and require separate analysis. Our main aim is to interpret all the data assuming the same physics (equation of state and superfluid properties) in the interiors of all neutron stars.

2 OBSERVATIONS

Table 1 summarizes the observations of isolated neutron stars, whose thermal surface radiation has been detected or constrained. We present the estimated stellar age t, effective surface temperature $T_{\rm s}^{\infty}$ and surface thermal luminosities $L_{\rm s}^{\infty}$ (as detected by a distant observer). The data on t and $T_{\rm s}^{\infty}$ are described by Gusakov et al. (2004a) in more detail, with two exceptions. First, following Slane et al. (2004b), we slightly lower the upper limit on the surface temperature $T_{\rm s}^{\infty}$ of PSR J0205+6449 in the supernova remnant 3C 58 ($T_{\rm s}^{\infty} < 1.02$ MK instead of 1.1 MK). Secondly, we include into consideration the central X-ray source RX J0007.0+7303 in the supernova remnant CTA 1.

For PSR J0205+6449 we adopt the age of the historical supernova SN 1181 ($t \approx 820$ yr). However, notice that recently Chevalier (2004, 2005) presented arguments in favour of a larger age of the pulsar wind nebula in 3C 58 ($t = 2400 \pm 500$ yr). Were this the actual age of the neutron star, its interpretation would be easier.

For the source RX J0007.0+7303 we adopt the age of its host supernova remnant CTA 1 (G119.5+10.2). According to Slane et al. (2004a), the age is $t = 13$ kyr. Following Halpern et al. (2004) we assume the neutron star age limits $10\,{\rm kyr} \lesssim t \lesssim 30\,{\rm kyr}$. As for RX J0205+6449, the Crab pulsar and RX J0007.0+7303, no thermal radiation component has been detected from these objects, and only the upper limits on $T_{\rm s}^{\infty}$ have been set (Weisskopf et al. 2004; Slane et al. 2004a,b; Halpern et al. 2004).

The surface temperatures of some sources from Table 1 (labelled by ^{c}) have been obtained by fitting their thermal radiation spectra with hydrogen atmosphere models. Such models are more consistent with other information on these sources (e.g. Pavlov & Zavlin 2003) than the blackbody model. For other sources (e.g. the Geminga pulsar and PSR B1055−52, labelled by ^{b}), we present the values of $T_{\rm s}^{\infty}$ inferred using the blackbody spectrum because this spectrum is more consistent for these sources. The surface temperature of RX J1856.4−3754 is still uncertain. Following Gusakov et al. (2004a) we adopt the upper limit $T_{\rm s}^{\infty} < 0.65$ MK. Finally, $T_{\rm s}^{\infty}$ for RX J0720.4−3125 is taken from Motch, Zavlin & Haberl (2003), who interpreted the observed spectrum with a model of a hydrogen atmosphere of finite depth. Note also the new results by Kargaltsev et al. (2005) for Geminga presented in Table 1. These authors confirm the observational value of $T_{\rm s}^{\infty}$ reported by Zavlin & Pavlov (2004). Taking into account systematic uncertainties of $T_{\rm s}^{\infty}$ discussed by Kargaltsev et al. (2005), we retain the 20 per cent error bars adopted by Gusakov et al. (2004a) and erroneously referred to as 90 per cent confidence level in their Table 1. Following Gusakov et al. (2004a), the same 20 per cent error bars will be adopted for PSR J0538+2817, PSR B1055−52 and RX J0720.4−3128.

As noted by several authors (e.g. Page et al. 2004), it may be instructive to compare the cooling theory with measured values of stellar thermal surface luminosities $L_{\rm s}^{\infty}$, rather than with $T_{\rm s}^{\infty}$. The data on $L_{\rm s}^{\infty}$ are also collected in Table 1. The luminosity is related to the effective surface temperature via

$$L_{\rm s}^{\infty} = 4\pi\sigma R_{\infty}^2 \left(T_{\rm s}^{\infty}\right)^4, \qquad (1)$$

where σ is the Stefan–Boltzmann constant, $R_{\infty} = R/\sqrt{1-2GM/(c^2R)}$ is the so-called apparent radius of a neutron star (as would be detected by a distant observer if a

Table 1. Observational limits on surface temperatures and thermal luminosities of isolated neutron stars.

Source	t (kyr)	$T_{\rm s}^{\infty}$ (MK)	Confidence (per cent)	References[a]	$\log L_{\rm s}^{\infty}$ (erg s^{-1})
PSR J0205+6449 (in 3C 58)	0.82	$<1.02^{b}$	99.8	S04b	<33.29
PSR B0531+21 (Crab)	1	$<2.0^{b}$	99.8	W04	<34.45
RX J0822−4300	2–5	1.6–1.9^{c}	90	ZTP99	33.9–34.2
1E 1207.4−5209	3–20	1.4–1.9^{c}	90	ZPS04	33.67–34.20
RX J0007.0+7303 (in CTA 1)	10–30	$<0.66^{b}$	–	H04	<32.54
PSR B0833−45 (Vela)	11–25	0.65–0.71^{c}	68	P01	32.19–32.67
PSR B1706−44	∼17	$0.82^{+0.01}_{-0.34}{}^{c}$	68	M04	31.66–32.94
PSR J0538+2817	30 ± 4	$\sim 0.87^{c}$	–	ZP04	32.32–33.33
PSR B0633+1748 (Geminga)	∼340	$\sim 0.5^{b}$	–	K05	31.34–32.37
RX J1856.4−3754	∼500	<0.65	–	G04a	<32.5
PSR B1055−52	∼540	$\sim 0.75^{b}$	–	PZ03	32.05–33.08
RX J0720.4−3125	∼1300	∼0.51	–	MZH03	31.37–32.40

[a]S04b, Slane et al. (2004b); W04, Weisskopf et al. (2004); ZTP99, Zavlin et al. (1999); ZPS04, Zavlin et al. (2004); H04, Halpern et al. (2004); P01, Pavlov et al. (2001); M04, McGowan et al. (2004); ZP04, Zavlin & Pavlov (2004); K05, Kargaltsev et al. (2005); G04a, see Gusakov et al. (2004a); PZ03, Pavlov & Zavlin (2003); MZH03, Motch et al. (2003).

[b]Inferred using the blackbody spectrum.

[c]Inferred using a hydrogen atmosphere model.

telescope could resolve the star), R is the circumferential radius, and M is the gravitational stellar mass. Thus, the luminosity is determined by the effective temperature and neutron star radius; an uncertainty in L_s^∞ is produced by uncertainties in T_s^∞ and R_∞. We have already described the values of T_s^∞. As for the values of R_∞, we vary them (with two exceptions indicated below) within the reasonable theoretical interval for neutron star radii, $R_\infty = 11$–16 km; while translating R into R_∞ we always set $M = 1.4\,M_\odot$.

In Table 1 the upper limits on L_s^∞ for PSR J0205+6449, the Crab pulsar, RX J0007.0+7303 and RX J1856.4−3754 were obtained assuming $R_\infty = 16$ km.

The luminosities of RX J0822−4300 and 1E 1207.4−5209 have been calculated from the values of T_s^∞ obtained by Zavlin, Trümper & Pavlov (1999) and Zavlin, Pavlov & Sanwal (2004), respectively. We have taken the same fixed radius $R = 10$ km ($R_\infty = 13$ km) as used by the cited authors to fit the observed spectra with the hydrogen atmosphere models. All other values of L_s^∞ in Table 1 have been obtained by varying R_∞ within the interval $R_\infty = 11$–16 km.

The central values of L_s^∞ have been calculated taking into account the central values of T_s^∞ from Table 1 and the values of R (or R_∞) obtained in the cited papers from spectral fits, except for the Vela pulsar, where we set $R_\infty = 13$ km. For PSR B1706−44, PSR J0538+2817 and RX J0720.4−3125, these values of R have been taken as 12, 10.5 and 10 km, as suggested by McGowan et al. (2004), Zavlin & Pavlov (2004) and Motch et al. (2003), respectively. For the Geminga pulsar we have used the value $R = 10.6$ km from Zavlin & Pavlov (2004), and for PSR B1055−52 we set $R = 13$ km from Pavlov & Zavlin (2003).

In all the cases, the limits of L_s^∞ presented in Table 1 seem to be rather uncertain. Although, in principle, the luminosities L_s^∞ can be measured or constrained more accurately than T_s^∞ (by exactly measuring the distance and the bolometric thermal flux), this is not so for the sources collected in Table 1 mainly due to large uncertainties in measured distances to the sources (see e.g. Page et al. 2004). Nevertheless, comparing observed and theoretical luminosities of cooling neutron stars seems to be useful. Our limits of L_s^∞ are in reasonable agreement with the corresponding limits given by Page et al. (2004). The main differences refer to the Geminga pulsar and 1E 1207.4−5209. In the first case the limits of L_s^∞ presented by Page et al. (2004) correlate with too low apparent radius of the star, $R_\infty < 6$ km, for the temperature limits adopted in their paper. In the second case, Page et al. used $L_s^\infty = L_s\,(R/R_\infty)^2$ with $L_s = 5.0^{+4.3}_{-1.8} \times 10^{33}$ erg s^{-1} from Zavlin, Pavlov & Trümper (1998). The value of L_s was possibly underestimated by Zavlin et al. (1998), because their value of T_s was indicated later by Zavlin et al. (2004) as T_s^∞.

Also, note that the radii of our neutron star models used for the cooling calculations presented below are consistent with the radii used for the interpretation of the data.

3 PHYSICS INPUT AND CALCULATIONS

The cooling calculations have been done using our general relativistic cooling code (Gnedin, Yakovlev & Potekhin 2001). At the initial cooling stage ($t \lesssim 100$ yr) the main cooling mechanism is neutrino emission, but the stellar interior stays highly non-isothermal. At the next stage (10^2 yr $\lesssim t \lesssim 10^5$ yr) neutrino emission is dominant, but the stellar interior is isothermal. Later ($t \gtrsim 10^5$ yr) the star cools predominantly through surface photon emission.

Following Gusakov et al. (2004a) we adopt the moderately stiff equation of state for the neutron star matter suggested by Douchin & Haensel (2001). In this case a neutron star core (a region of density $\rho > 1.3 \times 10^{14}$ g cm^{-3}) consists of neutrons with an admixture of protons, electrons and muons. All the constituents exist everywhere in the core, except for muons, which appear at $\rho > 2.03 \times 10^{14}$ g cm^{-3}. The most massive stable star has the (gravitational) mass $M = M_{\max} = 2.05\,M_\odot$, central density $\rho_c = 2.9 \times 10^{15}$ g cm^{-3} and (circumferential) radius $R = 9.99$ km. The parameters of neutron stars with some other masses are given by Gusakov et al. (2004a).

The employed equation of state forbids the powerful direct Urca process of neutrino emission (Lattimer et al. 1991) in all stable neutron stars ($M \leqslant M_{\max}$). Accordingly, a non-superfluid neutron star of any mass in the range $1\,M_\odot \lesssim M \leqslant M_{\max}$ (without any accreted envelope) will have almost the same (universal) cooling curve $T_s^\infty(t)$ (the dotted curve in the right-hand panel of Fig. 1). At the neutrino cooling stage, this curve is determined by the modified Urca process and is almost independent of the equation of state in the stellar core (see e.g. Yakovlev & Pethick 2004, and references therein). As seen from Fig. 1, this universal cooling curve cannot explain the data. We will show that all the data can be explained by assuming nucleon superfluidity in the internal layers of neutron stars and the presence of accreted envelopes (of light elements).

Following the standard procedure (Gudmundsson, Pethick & Epstein 1983), our code calculates heat transport in the neutron star interior ($\rho > \rho_b = 10^{10}$ g cm^{-3}) and uses the predetermined relation between the effective surface temperature T_s and the temperature T_b at the bottom of the surface heat-blanketing envelope ($\rho < \rho_b$). We use the relation calculated by Potekhin, Chabrier & Yakovlev (1997) and updated by Potekhin et al. (2003). We will employ the models of blanketing envelopes made of iron (which is the standard assumption) and envelopes containing light elements.

A detailed description of these models is given by Potekhin et al. (2003). The thermal energy in a heat-blanketing envelope is mainly conducted by electrons. The thermal conductivity of electrons that scatter off lighter ions in an accreted envelope is higher than the conductivity in an iron envelope. This means that an accreted envelope is more heat-transparent than an iron one, resulting in higher T_s for the same T_b. This rise in surface temperature depends on T_b and ΔM, the mass of light elements (hydrogen and/or helium, with a possible carbon/oxygen layer at the bottom of the accreted envelope as a result of nuclear burning of lighter elements). Potekhin et al. (1997, 2003) varied the boundaries of layers containing different elements within physically reasonable limits and found that the resulting relation between T_s and T_b is remarkably insensitive to these variations and depends mainly on ΔM. However, ΔM cannot exceed $\sim 10^{-7}\ M$, because at higher ΔM the bottom density of the accreted envelope would exceed 10^{10} g cm^{-3}. At such high densities, light elements (including carbon/oxygen) would rapidly transform into heavier ones.

At the neutrino cooling stage T_b is governed by neutrino emission from the stellar interior and is almost independent of the conductive properties in the heat-blanketing envelope. In contrast, at the photon cooling stage the star with the accreted envelope has lower T_b and, consequently, lower T_s due to the higher heat transparency of the surface layers. This leads to faster photon cooling through the surface (for not too cold stars; see e.g. Potekhin et al. 1997).

The cooling of a neutron star is sensitive to superfluidity of nucleons in the stellar core and to superfluidity of free neutrons in the inner stellar crust. Any superfluidity is characterized by its own density-dependent critical temperature $T_c(\rho)$. Microscopic theories predict mainly (i) singlet-state ($^1S_0$) pairing of neutrons ($T_c = T_{cns}$) in the inner crust and the outermost core, (ii) $^1S_0$ proton pairing in the core ($T_c = T_{cp}$), and (iii) triplet-state ($^3P_2$) neutron pairing in the core ($T_c = T_{cnt}$). These theories give a large

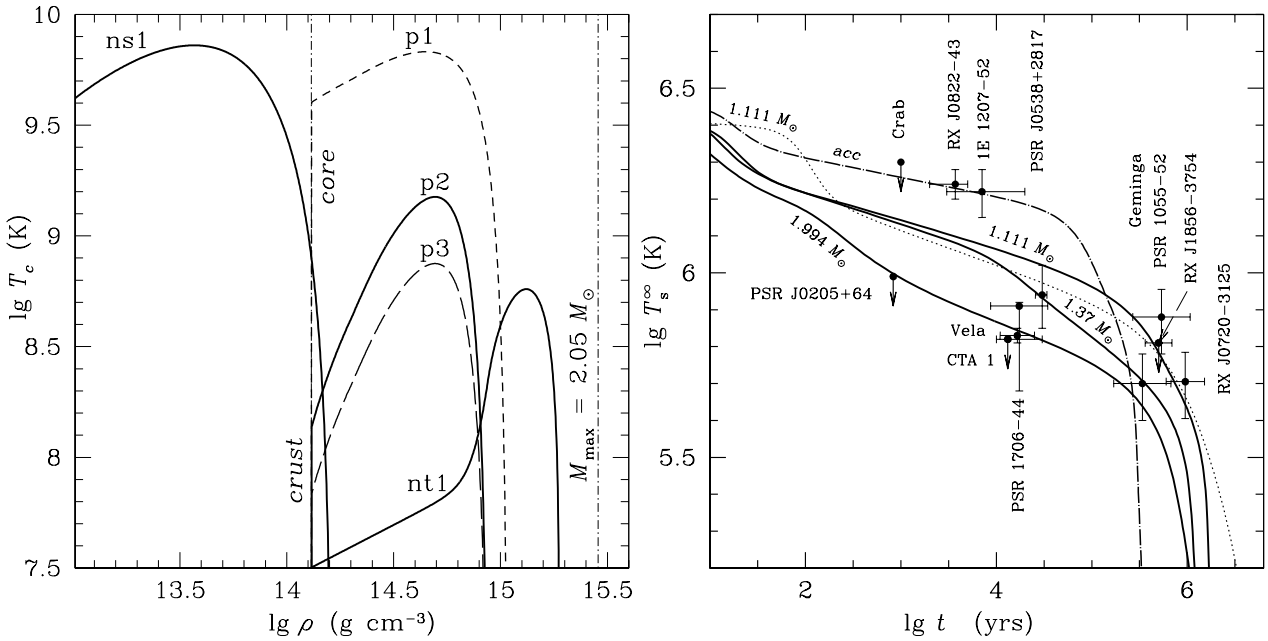

Figure 1. Left: density dependence of critical temperatures for the three models p1, p2 and p3 of singlet-state proton pairing and one model nt1 of triplet-state neutron pairing in the neutron star core, as well as model ns1 of singlet-state neutron pairing in the stellar crust. Vertical dot–dashed lines indicate the crust–core boundary and the central density of the maximum-mass neutron star. Right: observational limits of surface temperatures of neutron stars (Table 1) as compared with theoretical cooling curves. The three solid curves refer to neutron stars of different masses (indicated near the curves) with nucleon pairing p2, nt1 and ns1. The dot–dashed curve refers to an $M = 1.111\,\mathrm{M}_\odot$ neutron star with the same superfluidity, but with an accreted envelope of mass $\Delta M = 10^{-8}\ M$. The dotted curve is for a non-superfluid star of the same mass without any accreted envelope.

scatter of critical temperatures, from $\sim 10^{10}$ to $\sim 10^8$ K and lower, depending on the nucleon–nucleon interaction model and many-body theory employed (e.g. Yakovlev et al. 1999; Lombardo & Schulze 2001; see also recent papers by Schwenk & Friman 2004; Takatsuka & Tamagaki 2004; Zuo et al. 2004; Tanigawa et al. 2004). Because of these huge theoretical uncertainties, we will not rely on any specific microscopic results but will treat $T_{\rm cp}(\rho)$ and $T_{\rm cn}(\rho)$ as phenomenological functions of ρ (which can be varied within physically reasonable limits). Our aim will be to constrain these functions by comparing theoretical cooling curves with the observations.

Superfluidity of nucleons affects the heat capacity and suppresses neutrino processes such as Urca and nucleon–nucleon bremsstrahlung processes (as reviewed, for example, by Yakovlev et al. 1999). It also introduces an additional neutrino emission mechanism associated with the Cooper pairing of nucleons (Flowers, Ruderman & Sutherland 1976). All these effects of superfluidity are incorporated into our cooling code. While calculating the neutrino emission due to Cooper pairing of protons, we use phenomenological values of weak interaction parameters renormalized by many-body effects (the same as in Gusakov et al. 2004b).

In the left-hand panel of Fig. 1 we plot models for nucleon pairing adopted in our calculations: one model ns1 of strong singlet-state pairing of neutrons, with the peak of $T_{\rm cns}(\rho)$ approximately equal to $T_{\rm cns}^{\rm max} \approx 7 \times 10^9$ K; three models of proton pairing – strong p1, moderately strong p2 and moderate p3, with $T_{\rm cp}^{\rm max} \simeq 6.8 \times 10^9$, 1.5×10^9 and 7.5×10^8 K, respectively; and one model nt1 of moderate triplet-state neutron pairing, with $T_{\rm cn}^{\rm max} \sim 6 \times 10^8$ K. Models p1 and nt1 are the same as in Gusakov et al. (2004a). Now we add models of weaker proton pairing (particularly, p2). Strong proton pairing has been predicted in a number of publications (e.g. Tanigawa et al. 2004), while other publications predict much weaker proton pairing (e.g. Zuo et al. 2004; Takatsuka & Tamagaki 2004).

As seen in the right-hand panel of Fig. 1, proton pairing p2 combined with strong crustal superfluidity of neutrons ns1 results in too cold low-mass neutron stars. The neutrino emission due to Cooper pairing of protons in the core and of neutrons in the inner crust (see Section 4) accelerates the cooling and does not allow us to explain the observations of the young and hot neutron stars, RX J0822−4300 and 1E 1207.4−5209. However, this cooling scenario is consistent with the observations of the old and warm neutron stars, PSR 1055−52 and RX J0720.4−3125. Accreted envelopes can raise the surface temperatures of middle-aged neutron stars and explain the observations of RX J0822−4300 and 1E 1207.4−5209. This is demonstrated by the dot–dashed cooling curve for the low-mass star with accreted envelope of mass $\Delta M = 10^{-8}\ M$.

Our interpretation of the neutron stars coldest for their age (PSR J0205+6449 in 3C 58, RX J0007.0+7303 in CTA 1, and the Vela and Geminga pulsars) remains the same as in Gusakov et al. (2004a). These objects can be treated as massive neutron stars ($M \gtrsim 1.9\,\mathrm{M}_\odot$) with moderate triplet-state neutron pairing nt1 in their inner cores where proton pairing p1 (as well as p2 and p3) dies out (left-hand panel of Fig. 1). Our phenomenological pairing model nt1 seems specific (shifted to too high densities ρ). However, similar models have been obtained from microscopic theories (e.g. see the curve $m^* = 0.73$ in fig. 1 of Takatsuka & Tamagaki 1997).

In this way we come to the same three distinct classes of cooling neutron stars as in Gusakov et al. (2004a) (and generally as in Kaminker, Yakovlev & Gnedin 2002). The first class contains low-mass stars whose surface layers are composed of either iron or light elements (solid or dot–dashed cooling curves, respectively, for the $M = 1.111\,\mathrm{M}_\odot$ star in Fig. 1). Another class contains high-mass stars that show *enhanced* cooling (the solid curve for the $M = 1.994\,\mathrm{M}_\odot$ star) produced by neutrino emission due to the Cooper pairing of neutrons. Finally, there is a class of medium-mass neutron

stars (the solid curve for the $M = 1.37\,M_\odot$ star), which show intermediate cooling. Their cooling curves fill in the space between the upper curve for low-mass stars and the lower curve for high-mass stars. These curves explain the observations of PSR B1706−44, PSR J0538+2817 and RX J1856.4−3754.

4 COOLING OF LOW-MASS NEUTRON STARS

As shown in Section 3, the presence of light elements on the surfaces of the younger and hotter neutron stars, RX J0822−4300 and 1E 1207.4−5209, can allow us to explain their observations if we assume moderately strong proton pairing p2 in their interiors. This pairing is also consistent with the observations of the old and warmest sources, PSR B1055−52 and RX J0720.4−3125. We interpret all these sources as low-mass neutron stars. Let us analyse the main cooling regulators of such stars.

In our case, triplet-state neutron pairing in low-mass stars is weak. For the adopted equation of state of Douchin & Haensel (2001), this implies $T_{\rm cn}(\rho) \lesssim 2 \times 10^8$ K at $\rho \lesssim 8 \times 10^{14}\,{\rm g\,cm^{-3}}$. Under this condition, neutron pairing does not affect the cooling of low-mass stars ($M \lesssim 1.1\,M_\odot$) at least at the neutrino cooling stage. The thin short-dashed line in the left-hand panel of Fig. 2 shows that (in the absence of crustal pairing) strong proton pairing p1 is needed to explain the data on all neutron stars hottest for their age (Gusakov et al. 2004a). In contrast, cooling curves for moderately strong proton pairing p2 (thin solid line) and moderate pairing p3 (thin long-dashed line) go essentially lower than the curve for pairing p1, being inconsistent with the observations of RX J0822−4300 and 1E 1207.4−5209. More rapid cooling for these two models of proton superfluidity is provided by neutrino emission due to the Cooper pairing of protons that occurs at $t \sim 50$–100 yr.

The thick lines in the left-hand panel of Fig. 2 demonstrate the additional effect of neutron pairing ns1 in the crust. Comparing the three thick lines, one can see that crustal neutron pairing noticeably accelerates only very slow cooling of low-mass neutron stars with strong proton pairing p1 in their cores (Yakovlev, Kaminker & Gnedin 2001; Yakovlev et al. 2002). In that case the neutrino luminosity due to the Cooper pairing of neutrons in the stellar crust at $t \lesssim 3 \times 10^5$ yr may dominate the total neutrino luminosity of the stellar core. Moreover, at $t \gtrsim 3 \times 10^5$ yr crustal neutron pairing reduces the heat capacity of the crust. Both effects accelerate the cooling and decrease $T_{\rm s}^{\infty}$, violating the interpretation of the two hottest sources, RX J0822−4300 and 1E 1207.4−5209. Any model of weaker crustal superfluidity will only bring cooling curves closer to the thin ones and simplify the interpretation of the observations.

On the other hand, for moderately strong (p2) or moderate (p3) proton pairing in the core, the effects of strong crustal neutron pairing on the cooling of middle-aged neutron stars (10^3 yr $\lesssim t \lesssim 10^5$ yr) are almost negligible. Neutrino emission due to crustal Cooper pairing of neutrons can noticeably accelerate the cooling and decrease $T_{\rm s}^{\infty}$ only during the internal thermal relaxation stage ($t \lesssim 100$ yr).

The right-hand panel of Fig. 2 demonstrates that the observations of RX J0822−4300 and 1E 1207.4−5209 can be explained by adopting any model of proton pairing (p1, p2 or p3), model ns1 of crustal superfluidity, and the presence of an accreted envelope of mass $\Delta M = 10^{-8}\,M$ (thin lines).

Note that the upper dot–dashed cooling curve goes higher than is needed to interpret the observations of the young and hottest source RX J0822−4300. Accordingly, following Yakovlev et al. (2002) (see also Potekhin et al. 2003), we may assume the presence of a thinner accreted envelope (e.g. $\Delta M \sim 10^{-11}\,M_\odot$) to interpret the observations of RX J0822−4300 and 1E 1207.4−5209 (for the combination of p1 and ns1 pairing). The stronger the proton core superfluidity, the less massive accreted envelope is needed for the interpretation of the data for these two stars.

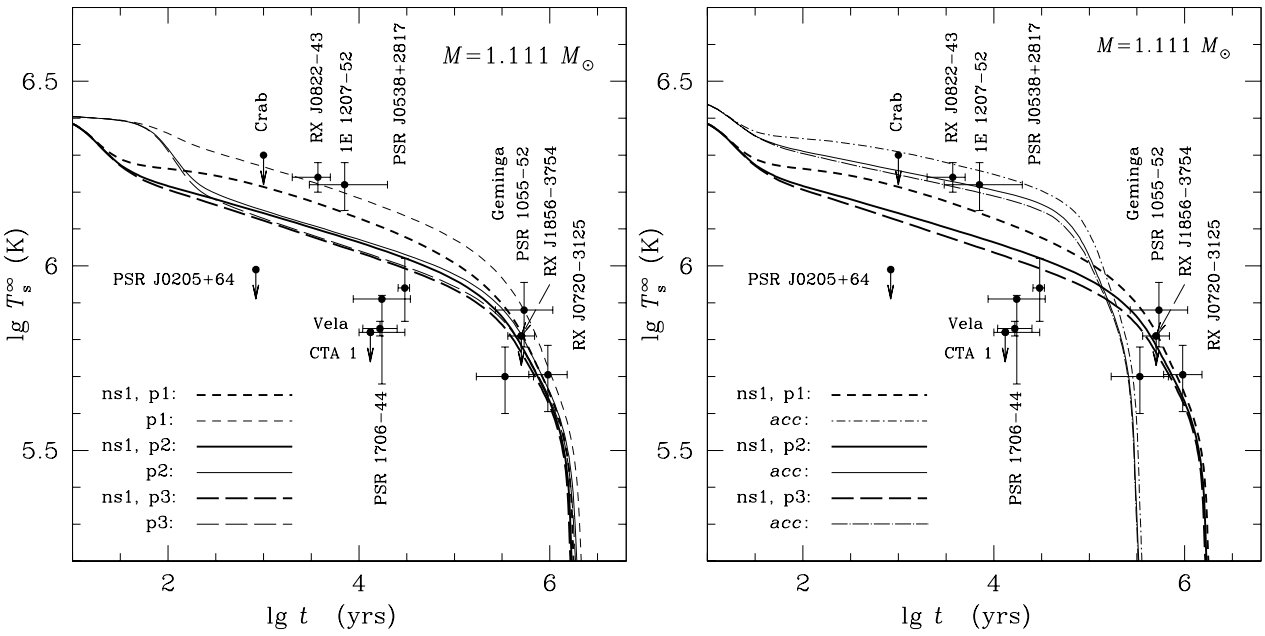

Figure 2. Cooling of low-mass ($1.111\,M_\odot$) neutron stars with proton pairing (models p1, p2 or p3) and neutron pairing nt1 (weak at low densities, Fig. 1) in the stellar core (thin short-dashed, solid and long-dashed curves, respectively), with the aim of interpreting the observations of neutron stars hottest for their age (RX J0822−4300, 1E 1207.4−5209, PSR B1055−52 and RX J0720.4−3125). The thick curves include, in addition, the effects of crustal neutron superfluidity ns1. Left: no accreted envelopes. Right: the thick curves are the same as in the left-hand panel. The thin dot–dashed and solid curves include, in addition, the effects of an accreted envelope of mass $\Delta M = 10^{-8}\,M$.

In order to explain the old and warmest sources, PSR B1055−52 and RX J0720.4−3125, we will treat them as low-mass stars with an iron surface and proton pairing p2 in the core (or a similar model of pairing with the peak of critical temperature $T_{\rm cp}^{\rm max} \gtrsim 10^9$ K). Moreover, the presence of any crustal neutron pairing (for example, ns1; thick solid lines in Fig. 2) does not violate the interpretation of these sources. Note that proton pairing p3 (thick long-dashed lines) is less appropriate for the interpretation of these sources than pairing p2. Therefore, we adopt proton pairing p2 as the basic model for a new cooling scenario. Obviously, any model of stronger proton pairing [with higher $T_{\rm cp}(\rho)$] is more consistent with the observations.

5 ACCRETED ENVELOPES AND COOLING OF NEUTRON STARS

Fig. 3 illustrates the effects of accreted envelopes of mass $\Delta M = 10^{-8}\,M$ on the cooling of neutron stars with different masses and the same nucleon pairing (models p2, nt1 and ns1). For comparison, we also present cooling curves for stars with an iron surface (thick solid lines) and the same nucleon superfluidity (see also the right-hand panel of Fig. 1). Note that the effect of crustal superfluidity on the cooling of such stars is unimportant.

In the left-hand panel of Fig. 3 we present our traditional cooling curves $T_{\rm s}^{\infty}(t)$ and compare them with data on surface temperature. In the right-hand panel we show the temporal evolution of the surface thermal luminosity $L_{\rm s}^{\infty}(t)$ and compare it with data (Table 1). The two representations of the same cooling processes are seen to be in reasonably good agreement, although the data on $L_{\rm s}^{\infty}$ are generally less certain and seem to be currently less conclusive (because, as a rule, the luminosity of the selected sources is determined less accurately than their surface temperature, as discussed in Section 2).

Fig. 3 shows a strong rise of the cooling curves for neutron stars with accreted envelopes at the neutrino cooling stage ($t \lesssim 3 \times 10^4$ yr) and their steep decrease at the photon cooling stage. Their photon stage starts earlier than for stars with an iron surface. Assuming the presence of accreted envelopes, we can explain the observations of the young and hottest neutron stars, RX J0822−4300 and 1E 1207.4−5209, treating them either as low-mass or as medium-mass stars. In contrast, the observations of the old and warmest objects, PSR B1055−52 and RX J0720.4−3125, can be explained only by treating them as low-mass stars with iron surfaces and with moderately strong (or strong) proton pairing inside.

It was shown by Chang & Bildsten (2003, 2004) that the mass of light elements may decrease with time, particularly due to diffusive nuclear burning. The characteristic burning time τ can be considered as an additional cooling regulator. Following Chang & Bildsten (2003, 2004) and Page et al. (2004) we assume that the mass of light elements decreases with time as $\Delta M\,(t) = \Delta M_0 \exp(-t/\tau)$, where ΔM_0 is the initial mass.

Fig. 4 illustrates the effect of variable mass of the accretion envelope on the cooling of an $M = 1.111\,{\rm M}_{\odot}$ neutron star. All the cooling curves are calculated assuming nucleon pairing p2, nt1 and ns1. The thick solid line is our typical cooling curve for a low-mass superfluid star without any accreted envelope. We use two values of the initial mass of light elements, $\Delta M_0/M = 10^{-9}$ and 10^{-7}, and thus present three pairs of cooling curves for three characteristic times τ. When τ is lower than the time of the transition from the neutrino cooling stage to the photon stage ($\tau < 3 \times 10^4$ yr), we obtain a smooth transition of the cooling track from the regime of highest temperatures in young stars to the regime of lower temperatures in old stars (cf. the curves for $M = 1.111\,{\rm M}_{\odot}$ in Figs 3 and 4). This effect has been pointed out by Page et al. (2004). At $\tau \gtrsim 3 \times 10^5$ yr, the cooling curves merge into the *limiting* curve obtained for constant $\Delta M = \Delta M_0$. In the intermediate case of $3 \times 10^4\,{\rm yr} \lesssim \tau \lesssim 3 \times 10^5$ yr, the cooling curves gradually approach this limiting curve with the increase of τ. As seen from Fig. 4, by

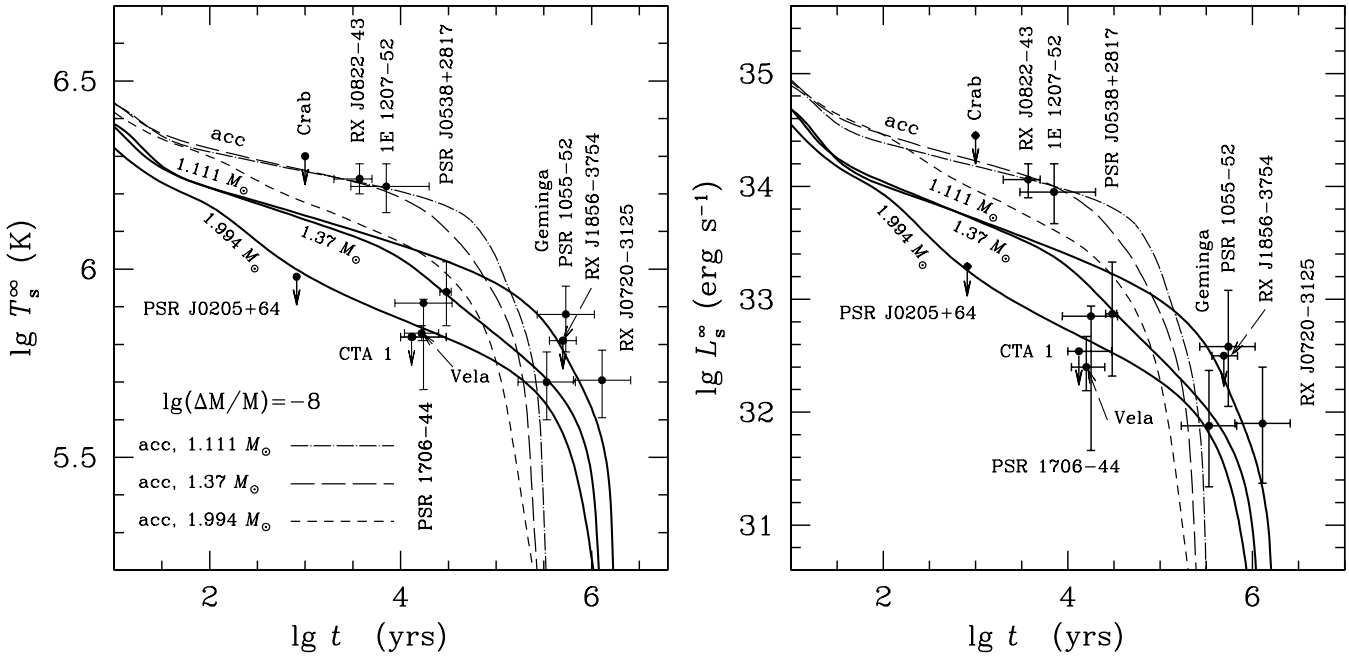

Figure 3. Cooling curves of neutron stars with different masses and nucleon pairing p2, nt1 and ns1 (Fig. 1) versus observations. The thin dot–dashed ($M = 1.111\,{\rm M}_{\odot}$), long-dashed ($M = 1.37\,{\rm M}_{\odot}$) and short-dashed ($M = 1.994\,{\rm M}_{\odot}$) curves are calculated including the effects of accreted envelopes ($\Delta M = 10^{-8}\,M$). The three thick solid curves are the same as the solid curves in the right-hand panel of Fig. 1. The left-hand and right-hand panels show the same cooling curves but as functions $T_{\rm s}^{\infty}(t)$ and $L_{\rm s}^{\infty}(t)$, respectively.

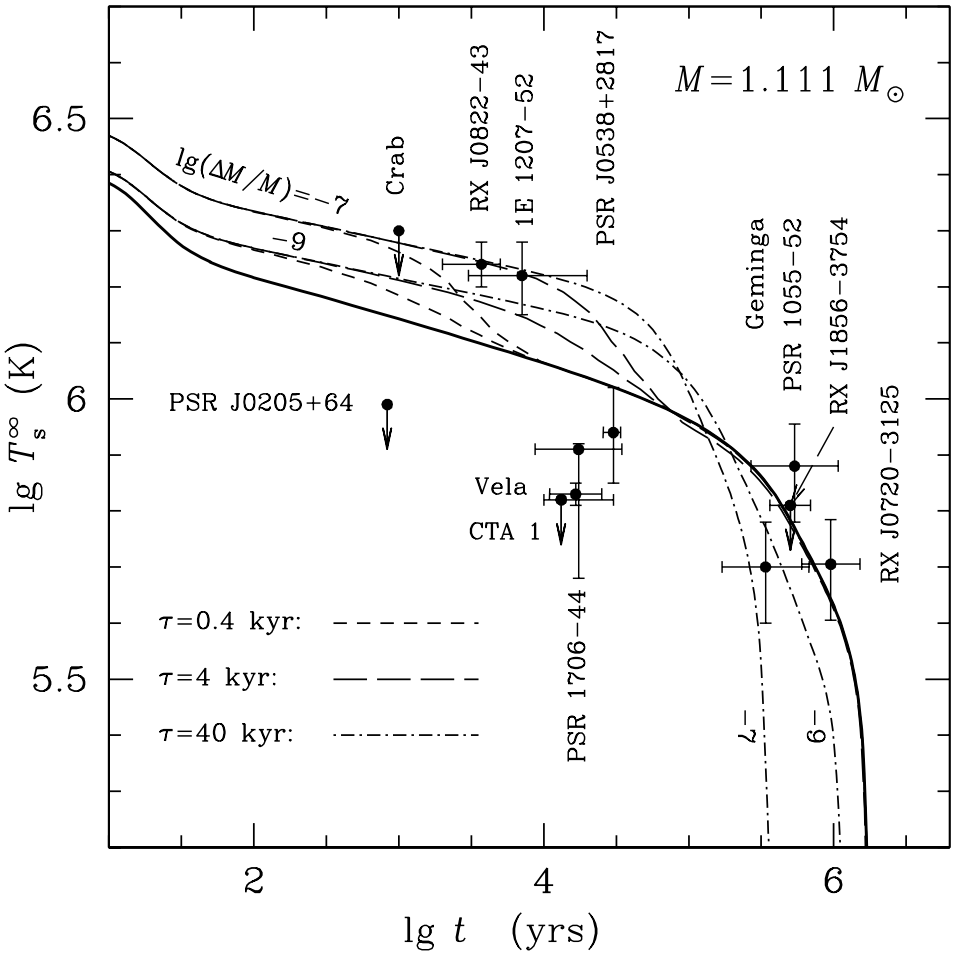

Figure 4. Cooling curves of 1.111-$M_\odot$ neutron stars with nucleon pairing p2, nt1 and ns1 versus observations. The thick solid curve is the same as in Fig. 3; the other curves are calculated assuming an exponential decay of accreted envelopes with characteristic times $\tau = 0.4$ kyr (short-dashed lines), 4 kyr (long-dashed lines) and 40 kyr (dot–dashed lines) for two values of the initial accreted mass, $\Delta M_0/M = 10^{-9}$ and 10^{-7}.

assuming any τ in the range $10^3 \lesssim \tau \lesssim 10^4$ yr, one can explain the observations of all neutron stars hottest for their age by one cooling curve. Note also that the value $\Delta M_0/M = 10^{-9}$ is too small to explain the observations of the young and hottest neutron stars, especially RX J0822−4300, at any τ.

As remarked by Chang & Bildsten (2004), the accreted envelope of a pulsar can become thinner owing to the excavation of ions from the stellar surface by a pulsar wind at a rate $\dot{M} \sim 2\Omega^2 m_\mathrm{i}\mu/ec$, where Ω is the pulsar spin frequency, μ is the magnetic moment and m_i is the ion mass. For an ordinary pulsar with spin period ∼0.1 s, $\mu \sim 10^{30}$ G cm^3, and for a helium surface we would have a surface mass loss $\Delta M_\mathrm{ex} \sim 6 \times 10^{-12}\,\mathrm{M}_\odot$ in $t \sim 10^5$ yr, too small to affect the cooling of a star with an initial helium layer of $\Delta M \gtrsim 10^{-10}\,\mathrm{M}_\odot$. For a pulsar with much higher magnetic field and/or faster rotation, the effect may be stronger and affect the cooling.

6 CONCLUSIONS

We have extended the scenario of neutron star cooling proposed by Gusakov et al. (2004a) by taking into account the effects of accreted envelopes and crustal singlet-state pairing of neutrons. As already stressed in Section 1, this scenario is different from the minimal cooling scenario of Page et al. (2004).

The general idea of the minimal cooling scheme is that the enhanced neutrino emission, required to interpret the observations of neutron stars coldest for their age, is provided by neutrino emission due to the Cooper pairing of neutrons. In this case the direct Urca process or similar enhanced neutrino processes in kaon-condensed, pion-condensed, or quark matter can be forbidden in neutron stars of all masses.

As in Gusakov et al. (2004a), the proposed cooling scenario imposes stringent constraints on the density dependence of the critical temperature $T_\mathrm{cn}(\rho)$ for triplet-state neutron pairing in the stellar core. They result from the comparison of theoretical cooling curves with data on the three most important 'testing sources', PSR J0205+6449, RX J0007.0+7303 and the Vela pulsar (Section 3). By tuning our phenomenological model of triplet-state neutron pairing in the stellar core, we obtain a noticeable dependence of the cooling on neutron star mass. This enables us to explain all the data by a single combination of models for nucleon superfluidity. Assuming the presence of accreted envelopes, we obtain two additional parameters to regulate the cooling, which are the initial envelope mass ΔM_0 and its characteristic burning time τ (Chang & Bildsten 2003).

Our interpretation implies the presence of moderately strong proton pairing ($T_\mathrm{cp}^\mathrm{max} \gtrsim 10^9$ K) and moderate triplet-state neutron pairing

(with $T_{\rm cnt}^{\rm max} \sim 6 \times 10^8$ K) in neutron star cores. Also, we have taken into account the effect of strong singlet-state neutron pairing ($T_{\rm cns}^{\rm max} \sim 7 \times 10^9$ K) in the stellar crust. However, as shown in Sections 4 and 5, the effect of crustal superfluidity is unimportant for cooling middle-aged neutron stars with moderately strong proton pairing in their cores.

We need proton superfluidity to explain the observations of the neutron stars hottest for their age. However, in contrast to the cooling scenario of Gusakov et al. (2004a), our new cooling scenario does not require too strong proton pairing. In fact, we can explain the observations of the old and warmest stars, PSR B1055−52 and RX J0720.4−3125, by treating them as low-mass neutron stars (without accreted envelopes) with moderately strong proton pairing in their cores. Such phenomenological models for proton pairing are consistent with recent microscopic calculations of proton critical temperatures by Zuo et al. (2004) and Takatsuka & Tamagaki (2004).

The young and hottest neutron stars, RX J0822−4300 and 1E 1207.4−5209, can also be treated as low-mass stars with the same moderate proton superfluidity in their cores but assuming the presence of accreted envelopes. The smaller the mass of the envelope, required for the interpretation of these sources, the stronger proton pairing should be assumed.

As discussed above, we need neutron pairing nt1 (or similar) to explain the observations of the stars coldest for their age. However, as demonstrated by Gusakov et al. (2004b), the cooling curves are not too sensitive to exchanging neutron and proton superfluidities [$T_{\rm cp}(\rho) \rightleftharpoons T_{\rm cn}(\rho)$] in neutron star cores. Therefore, we would also be able to explain the data in the scenario with moderately strong neutron and moderate proton pairing in the stellar cores.

Neutron star cooling can also be affected by surface magnetic fields and by some reheating mechanisms in neutron star interiors. We have not discussed the effects of magnetic fields (although they are incorporated in our cooling code). The main reason is that these effects are weaker than the effects discussed above [for ordinary cooling of isolated neutron stars of non-magnetar type; see e.g. Yakovlev et al. (2002) for a detailed discussion of this point]. Internal reheating mechanisms (see e.g. Page 1998a,b, and references therein), for instance, reheating due to the viscous dissipation of differential rotation, are relatively weak and model-dependent; they become important at the photon cooling stage. No reheating is required to explain the data in our cooling scenario. What is more important is that most elaborated model equations of state of dense matter (Akmal, Pandharipande & Ravenhall 1998) predict the operation of the direct Urca process in most massive stable neutron stars. This should lead to the existence of new classes of cooling neutron stars. The scenario with the open direct Urca process (which can be called the *extended minimal cooling scenario*) has been studied by Gusakov et al. (2005).

It is important that the same physics of neutron star interiors, which is tested by observations of isolated (cooling) neutron stars, can also be tested by observations of accreting neutron stars in soft X-ray transients (e.g. Yakovlev, Levenfish & Haensel 2003) based on the hypothesis of deep crustal heating of such stars (Brown, Bildsten & Rutledge 1998) by pycnonuclear reactions in accreted matter (Haensel & Zdunik 1990). The observations of soft X-ray transients in quiescent states indicate (Yakovlev, Levenfish & Gnedin 2005) the existence of rather cold neutron stars (first of all, SAX J1808.4−3658) inconsistent with the model of neutron star structure proposed in the present paper. However, these observational indications are currently inconclusive (e.g. Yakovlev et al. 2005). If confirmed in future observations, they could give stronger evidence against the proposed scenario than new observations of cooling neutron stars. In this case the extended minimal cooling scenario may appear to be more perspective.

ACKNOWLEDGMENTS

We are grateful to Yurii Shibanov for very fruitful discussions and critical remarks, and to Patrick Slane for useful discussion of the observational data. This work was supported partly by the RFBR (grants 03-07-90200, 05-02-22003, 05-02-16245), by the Russian Leading Science Schools (grant 1115.2003.2), by the Russian Science Support Foundation, and by the INTAS (grant YSF 03-55-2397).

REFERENCES

Akmal A., Pandharipande V. R., Ravenhall D. G., 1998, Rhys. Rev. C, 58, 1804
Brown E. F., Bildsten L., Rutledge R. E., 1998, ApJ, 504, L95
Chang P., Bildsten L., 2003, ApJ, 585, 464
Chang P., Bildsten L., 2004, ApJ, 605, 830
Chevalier R. A., 2004, Adv. Space Res., 33, 456
Chevalier R. A., 2005, ApJ, 619, 839
Douchin F., Haensel P., 2001, A&A, 380, 151
Flowers E. G., Ruderman M., Sutherland P. G., 1976, ApJ, 205, 541
Gnedin O. Y., Yakovlev D. G., Potekhin A. Y., 2001, MNRAS, 324, 725
Gudmundsson E. H., Pethick C. J., Epstein R. I., 1983, ApJ, 272, 286
Gusakov M. E., Kaminker A. D., Yakovlev D. G., Gnedin O. Y., 2004a, A&A, 423, 1063
Gusakov M. E., Kaminker A. D., Yakovlev D. G., Gnedin, O. Y., 2004b, Astron. Lett., 30, 759
Gusakov M. E., Kaminker A. D., Yakovlev D. G., Gnedin, O. Y., 2005, MNRAS, 363, 563
Haensel P., Zdunik J. L., 1990, A&A, 227, 431
Halpern J. P., Gotthelf E. V., Camilo F., Helfand D. J., Ransom S. M., 2004, ApJ, 612, 398
Kaminker A. D., Haensel P., Yakovlev D. G., 2001, A&A, 373, L17
Kaminker A. D., Yakovlev D. G., Gnedin O. Y., 2002, A&A, 383, 1076
Kargaltsev O. Y., Pavlov G. G., Zavlin V. E., Romani R. W., 2005, ApJ, 625, 307
Lattimer J. M., Pethick C. J., Prakash M., Haensel P., 1991, Phys. Rev. Lett., 66, 2701
Lombardo U., Schulze H.-J., 2001, in Blaschke D., Glendenning N. K., Sedrakian A., eds, Physics of Neutron Star Interiors. Springer, Berlin, p. 30
McGowan K. E., Zane S., Cropper M., Kennea J. A., Córdova F. A., Ho C., Sasseen T., Vestrand W. T., 2004, ApJ, 600, 343
Motch C., Zavlin V. E., Haberl F., 2003, A&A, 408, 323
Page D., 1998a, in Buccheri R., van Paradijs J., Alpar M. A., eds, The Many Faces of Neutron Stars. Kluwer, Dordrecht, p. 539
Page D., 1998b, in Shibazaki N., Kawai N., Shibata S., Kifune T., eds, Neutron Stars and Pulsars. Universal Academy Press, Tokyo, p. 183
Page D., Lattimer J. M., Prakash M., Steiner A. W., 2004, ApJS, 155, 623
Pavlov G. G., Zavlin V. E., 2003, in Bandiera R., Maiolino R., Mannucci F., eds, XXI Texas Symp. on Relativistic Astrophysics, Texas in Tuscany. World Scientific, Singapore, p. 319
Pavlov G. G., Zavlin V. E., Sanwal D., Burwitz V., Garmire G. P., 2001, ApJ, 552, L129
Pavlov G. G., Zavlin V. E., Sanwal D., 2002, in Becker W., Lesh H., Trümper J., eds, 270 WE-Heraeus Seminar on Neutron Stars, Pulsars and Supernova Remnants. MPE, Garching, p. 273
Potekhin A. Y., Chabrier G., Yakovlev D. G., 1997, A&A, 323, 415
Potekhin A. Y., Yakovlev D. G., Chabrier G., Gnedin O. Y., 2003, ApJ, 594, 404
Schwenk A., Friman B., 2004, Phys. Rev. Lett., 92, 082501

Slane P., Zimmerman E. R., Hughes J. P., Seward F. D., Gaensler B. M., Clarke M. J., 2004a, ApJ, 601, 1045
Slane P., Helfand D. J., Van der Swaluw E., Murray S. S., 2004b, ApJ, 616, 403
Takatsuka T., Tamagaki R., 1997, Prog. Theor. Phys., 97, 345
Takatsuka T., Tamagaki R., 2004, Nucl. Phys. A, 738, 387
Tanigawa T., Matsuzaki M., Chiba S., 2004, Phys. Rev. C, 70, 065801
Weisskopf M. C., O'Dell S. L., Paerels F., Elsner R. F., Becker W., Tennant A. F., Swartz D. A., 2004, ApJ, 601, 1050
Yakovlev D. G., Pethick C. J., 2004, ARA&A, 42, 169
Yakovlev D. G., Levenfish K. P., Shibanov Yu. A., 1999, Sov. Phys. – Usp., 42, 737
Yakovlev D. G., Kaminker A. D., Gnedin O. Y., 2001, A&A, 379, L5
Yakovlev D. G., Gnedin O. Y., Kaminker A. D., Potekhin A. Y., 2002, in Becker W., Lesh H., Trümper J., eds, 270 WE-Heraeus Seminar on Neutron Stars, Pulsars and Supernova Remnants. MPE, Garching, p. 287
Yakovlev D. G., Levenfish K. P., Haensel P., 2003, A&A, 407, 265
Yakovlev D. G., Levenfish K. P., Gnedin O. Y., 2005, Eur. Phys. J. A, 25, s01, 669
Zavlin V. E., Pavlov G. G., 2004, Mem. Soc. Astron. Ital., 75, 485
Zavlin V. E., Pavlov G. G., Trümper J., 1998, A&A, 331, 821
Zavlin V. E., Trümper J., Pavlov G. G., 1999, ApJ, 525, 959
Zavlin V. E., Pavlov G. G., Sanwal D., 2004, ApJ, 606, 444
Zuo W., Li Z. H., Lu G. C., Li J. Q., Scheid W., Lombardo U., Schulze H.-J., Shen C. W., 2004, Phys. Lett. B, 595, 44

This paper has been typeset from a TEX/LATEX file prepared by the author.